

NuSTAR Discovery of Dead Quasar Engine in Arp 187

著者	Kohei Ichikawa, Taiki Kawamuro, Megumi Shidatsu, Claudio Ricci, Hyun-Jin Bae, Kenta Matsuoka, Jaejin Shin, Yoshiki Toba, Junko Ueda, Yoshihiro Ueda
journal or publication title	The Astrophysical Journal Letters
volume	883
number	1
page range	L13
year	2019-09-19
URL	http://hdl.handle.net/10097/00128293

doi: 10.3847/2041-8213/ab3ebf



NuSTAR Discovery of Dead Quasar Engine in Arp 187

Kohei Ichikawa^{1,2}, Taiki Kawamuro³, Megumi Shidatsu⁴, Claudio Ricci^{5,6}, Hyun-Jin Bae⁷, Kenta Matsuoka⁸,
Jaejin Shin⁹, Yoshiki Toba^{8,10,11}, Junko Ueda^{3,12}, and Yoshihiro Ueda¹⁰

¹ Frontier Research Institute for Interdisciplinary Sciences, Tohoku University, Sendai 980-8578, Japan; k.ichikawa@astr.tohoku.ac.jp

² Astronomical Institute, Tohoku University, Aramaki, Aoba-ku, Sendai, Miyagi 980-8578, Japan

³ National Astronomical Observatory of Japan, 2-21-1 Osawa, Mitaka, Tokyo 181-8588, Japan; taiki.kawamuro@nao.ac.jp

⁴ Department of Physics, Faculty of Science, Ehime University, Matsuyama 790-8577, Japan

⁵ Núcleo de Astronomía de la Facultad de Ingeniería, Universidad Diego Portales, Av. Ejército Libertador 441, Santiago, Chile

⁶ Kavli Institute for Astronomy and Astrophysics, Peking University, Beijing 100871, People's Republic of China

⁷ Department of Medicine, University of Ulsan College of Medicine, Seoul 05505, Republic of Korea

⁸ Research Center for Space and Cosmic Evolution, Ehime University, 2-5 Bunkyo-cho, Matsuyama, Ehime 790-8577, Japan

⁹ Astronomy Program, Department of Physics and Astronomy, Seoul National University, Seoul, 151-742, Republic of Korea

¹⁰ Department of Astronomy, Kyoto University, Kitashirakawa-Oiwake-cho, Sakyo-ku, Kyoto 606-8502, Japan

¹¹ Academia Sinica Institute of Astronomy and Astrophysics, 11F of Astronomy-Mathematics Building, AS/NTU, No.1, Section 4, Roosevelt Road, Taipei 10617, Taiwan

¹² Harvard-Smithsonian Center for Astrophysics, 60 Garden Street, Cambridge, MA 02138, USA

Received 2019 August 6; revised 2019 August 26; accepted 2019 August 27; published 2019 September 19

Abstract

Recent active galactic nucleus (AGN) and quasar surveys have revealed a population showing rapid AGN luminosity variability by a factor of ~ 10 . Here we present the most drastic AGN luminosity decline by a factor of $\gtrsim 10^3$ constrained by a *NuSTAR* X-ray observation of the nearby galaxy Arp 187, which is a promising “dead” quasar whose current activity seems quiet but whose past activity of $L_{\text{bol}} \sim 10^{46} \text{ erg s}^{-1}$ is still observable at a large scale by its light echo. The obtained upper bound of the X-ray luminosity is $\log(L_{2-10 \text{ keV}}/\text{erg s}^{-1}) < 41.2$, corresponding to $\log(L_{\text{bol}}/\text{erg s}^{-1}) < 42.5$, indicating an inactive central engine. Even if a putative torus model with $N_{\text{H}} \sim 1.5 \times 10^{24} \text{ cm}^{-2}$ is assumed, the strong upper bound still holds with $\log(L_{2-10 \text{ keV}}/\text{erg s}^{-1}) < 41.8$ or $\log(L_{\text{bol}}/\text{erg s}^{-1}) < 43.1$. Given the expected size of the narrow-line region, this luminosity decrease by a factor of $\gtrsim 10^3$ must have occurred within $\lesssim 10^4 \text{ yr}$. This extremely rapid luminosity/accretion shutdown is puzzling, and it requires one burst-like accretion mechanism producing a clear outer boundary for an accretion disk. We raise two possible scenarios realizing such an accretion mechanism: a mass accretion (1) by the tidal disruption of a molecular cloud and/or (2) by the gas depletion as a result of vigorous nuclear star formation after rapid mass inflow to the central engine.

Unified Astronomy Thesaurus concepts: Active galactic nuclei (16); X-ray active galactic nuclei (2035)

1. Introduction

One of the fundamental questions on supermassive black holes (SMBHs) is how they stop growing their mass. The recent and ongoing quasar surveys have revealed massive SMBHs with masses of $M_{\text{BH}} \gtrsim 10^9 M_{\odot}$ at $z > 7$ (e.g., Mortlock et al. 2011), and interestingly, there seems to be a redshift-independent maximum mass limit at $M_{\text{BH}} \sim 10^{10.5} M_{\odot}$ (e.g., Netzer 2003; Kormendy & Ho 2013). This suggests that there is a fundamental quenching mechanism of the SMBH growth independently from the cosmic evolution, and possible mechanisms have been discussed theoretically by several authors (e.g., Natarajan & Treister 2009; Inayoshi & Haiman 2016; King 2016).

However, it is still observationally difficult to find quasars in the final growing/dying phase. The Soltan argument requires the total active galactic nucleus (AGN) lifetime is the order of 10^{7-9} yr (Soltan 1982; Marconi et al. 2004), and even a single episode of AGN activity should be longer than 10^5 yr (Schawinski et al. 2015), and possibly 10^{6-7} yr (e.g., Marconi et al. 2004; Hopkins et al. 2006). This long lifetime implies that it is extremely difficult to witness the “newly born” or “dying” phase of each AGN within the human timescale of $\lesssim 100 \text{ yr}$.

One solution for this issue is using the difference in the physical size among AGN indicators, some of which would give us the quasar time variability longer than the human

timescale. AGN have multiple indicators with different physical scales from 10 to $100 R_{\text{g}}$ (X-ray corona and UV–optically bright accretion disk; Dai et al. 2010; Morgan et al. 2010), ~ 0.1 –10 pc (AGN tori; Bartscher et al. 2013; Ichikawa et al. 2015), to ~ 1 –10 kpc (narrow-line region, NLR, or AGN jet; O’Dea 1998; Bennert et al. 2002), and the luminosities of the AGN indicators are tightly correlated with each other (Ichikawa et al. 2012, 2017, 2019a; Toba et al. 2014; Asmus et al. 2015; Ueda et al. 2015). Recent observations have revealed an interesting AGN population that shows strong AGN activity at large scales with $\sim 1 \text{ kpc}$ but much weaker one at small scales ($< 10 \text{ pc}$), suggesting a fading activity of the central engine. They are called fading AGN and currently ~ 20 such sources have been reported (e.g., Schirmer et al. 2013; Ichikawa et al. 2016, 2019b; Kawamuro et al. 2017; Keel et al. 2017; Villar-Martín et al. 2018; Sartori et al. 2018; Wylezalek et al. 2018).

Out of those ~ 20 sources, Arp 187, a merger remnant infrared galaxy located at $z = 0.04$ ($D_L = 178 \text{ Mpc}$), is the most promising “dying” or “dead” quasar candidate, which completely lacks current AGN signatures on small scales ($< 10 \text{ pc}$), but previous AGN activity estimated by the large-scale AGN indicators ($\gtrsim 1 \text{ kpc}$) must have reached quasar level luminosity. Previous VLA and ALMA 5–100 GHz radio observations have revealed the bimodal jet lobes with $\sim 5 \text{ kpc}$ size, whose kinematic jet age is $8 \times 10^4 \text{ yr}$. On the

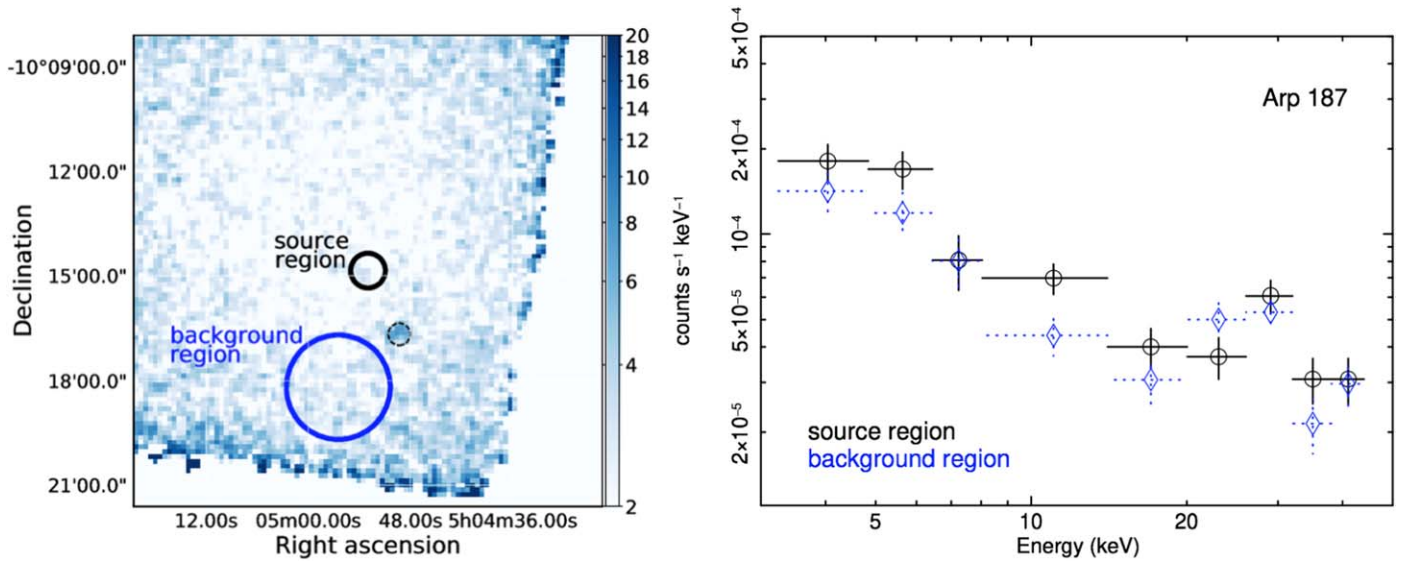


Figure 1. (Left) The exposure-corrected 8–24 keV image of *NuSTAR* in units of 10^{-6} counts s^{-1} pixel $^{-1}$. This was created by combining the FPMA and FPMB data. The source/background region of Arp 187 is shown with black/blue solid circles, respectively. The small dashed black circle represents an X-ray source, whose counterpart is likely to be GALEXASC J050449.00-101633.6, but is not our target Arp 187 (see the text for more details). (Right) The *NuSTAR* 3–50 keV spectra of the source and background regions (the black and blue circles in the left panel), indicated by the black solid and blue dotted bins, respectively.

other hand, the central radio-core is absent, suggesting that the central engine is already faint or even quenched. The optical spectrum indicates that Arp 187 has a narrow-line region with an estimated size of ~ 1 kpc, and the expected AGN luminosity reaches $L_{\text{bol}} = 1.5 \times 10^{46}$ erg s^{-1} (Ichikawa et al. 2019b). On the small scale, ~ 10 pc AGN torus emission was not detected in the *Spitzer*/IRS mid-infrared spectrum, whose emission is dominated by the host galaxy, suggesting the absence of the current AGN torus activity with the upper bound of $L_{\text{bol}} < 6 \times 10^{43}$ erg s^{-1} (Ichikawa et al. 2016).

However, we still lack a strong constraint on the current activity. In this Letter, we report the first *NuSTAR* hard X-ray observation for this target. Thanks to its strong penetration power against absorption, *NuSTAR* puts the strongest constraint on the current AGN luminosity even in the case of heavy obscuration, allowing us to conclude that Arp 187 has an inactive central engine.

2. *NuSTAR* Observations and Results

The *NuSTAR* data were obtained with an on-source exposure of 82 ks (GO cycle-4 Program 04037, PI: K. Ichikawa). Following the “*NuSTAR* Analysis Quickstart¹³ Guide,” we reprocessed the data from the *NuSTAR* detector modules of FPMA and FPMB with the standard *NuSTAR* script of nupipeline, which has two options to remove times with a high background (i.e., saamode and tentable). From the telemetry report on count rates over the focal plane, we found slightly higher rates in orbits around the standard SAA area (~ 2 counts s^{-1}) than typical values ($\lesssim 1$ count s^{-1}). Thus, saamode=optimized was adopted. Even if a more strict option of saamode=strict is used, our conclusion is unchanged. By contrast, such an increase cannot be clearly seen in the so-called tentacle region (Forster et al. 2014) near the SAA, but by following recommendation of the *NuSTAR* team, we adopted tentacle=yes. An alternative option of

tentable=no indeed provides a similar result, thus having little impact on our conclusion. The left panel of Figure 1 shows an exposure-corrected 8–24 keV image, created by combining the FPMA and FPMB data and smoothed by a Gaussian function with $\sigma = 2$ pixels.

As indicated in the X-ray image, we defined a source region as a circle with a $30''$ radius centered at the optical position of the galaxy, and the background region was selected from the same chip as an off-source area with a $90''$ radius. The larger size was set to avoid local statistical fluctuations of the background level. We confirm an insignificant change of our conclusion, even if a background spectrum is taken from a $30''$ circle near the source region. Note that, in the field of view, an X-ray source was serendipitously detected in (R.A., decl.) \sim (05: 04: 49.325, $-10: 16: 40.17$) with $\approx 8.8\sigma$ significance at 8–24 keV, and its counterpart is likely to be GALEXASC J050449.00–101633.6 at (05: 04: 49.0, $-10: 16: 33.7$). Its 2–10 keV flux estimated by a power-law model fit is $\sim 7 \times 10^{-14}$ erg cm^{-2} s^{-1} . Given its location far from our target Arp 187 with an angular separation of $\approx 2'$, which is at least six times larger than the positional uncertainty of *NuSTAR* (up to $\approx 20''$; e.g., Lansbury et al. 2017), we conclude that the emission does not originate from Arp 187, and hereafter we will not discuss this source.

The right panel of Figure 1 shows obtained spectra at 3–50 keV from the two regions in the left panel. The source spectrum shows no significant excess (2.9σ and 1.5σ in the 3.0–8.0 keV and 8.0–24 keV bands, respectively) to the background one. By considering an unabsorbed cutoff power-law component with the photon index of 1.7 and cutoff energy of 360 keV (Kawamuro et al. 2016),¹⁴ the 3σ upper limits of the 8–24 keV flux and luminosity are estimated to be 3.8×10^{-14} erg cm^{-2} s^{-1} and 1.4×10^{41} erg s^{-1} , equivalent to the 2–10 keV luminosity of 1.6×10^{41} erg s^{-1} , corresponding to

¹³ https://heasarc.gsfc.nasa.gov/docs/nustar/analysis/nustar_quickstart_guide.pdf

¹⁴ Even if we adopt another plausible parameter set of $\Gamma = 1.8$ and cutoff energy of 200 keV, found for a large, hard X-ray-selected AGN sample by Ricci et al. (2017), the upper limit of the 2–10 keV luminosity increases only by $\approx 10\%$, thus having little impact on our conclusion.

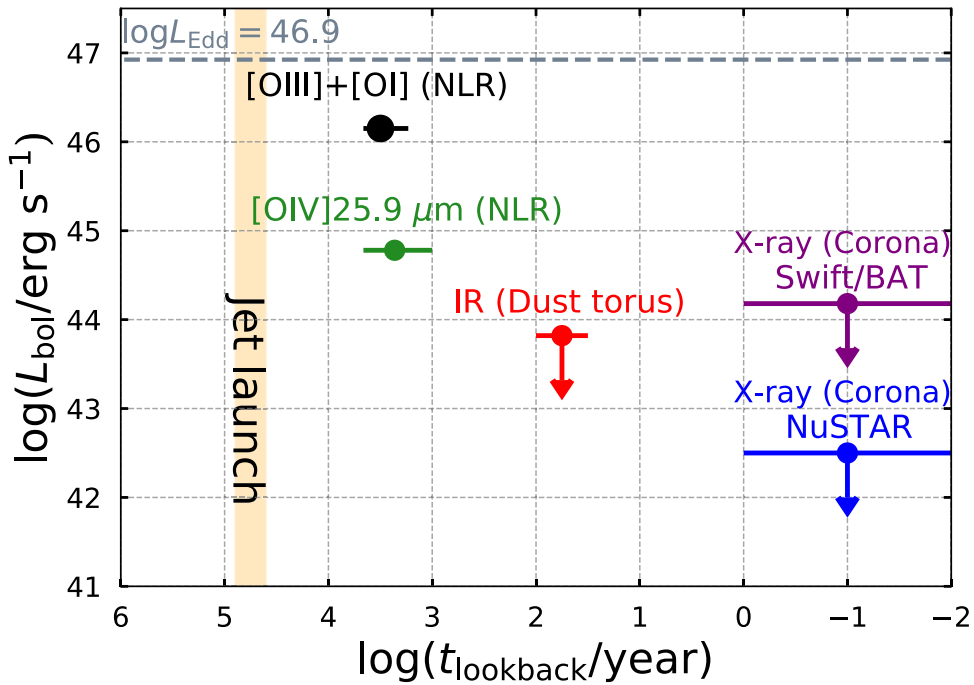


Figure 2. Long-timescale light curve of Arp 187 based on the AGN indicators with multiple physical scales. The estimated lookback time is based on the light-crossing time of each emission region. All except the blue point are taken from Ichikawa et al. (2016, 2019b). The black/green point is obtained from the optical [O III] λ 5007+[O I] λ 6300 emission line and [O IV]25.89 μ m emission. The red point is obtained from the *Spitzer*/IRS spectra, and the purple one is the previously obtained X-ray upper bound from the *Swift*/BAT hard X-ray survey. The blue point shows the upper-bound luminosity obtained by *NuSTAR* in this study. The 3σ upper bounds are shown for the IR and X-ray observations. The “jet launch” time (orange area) is estimated by $t_{\text{lookback}} = 8 \times 10^4$ yr from the kinetic age of the jet lobe assuming its typical expansion speed of $v = 0.1c$.

$L_{\text{bol}} < 3.2 \times 10^{42} \text{ erg s}^{-1}$ with a bolometric correction factor of 20 (Vasudevan et al. 2009). Hereafter, all upper limits on X-ray fluxes are at the 3σ level. This estimate is not so sensitive to absorption in the sight line up to $\log(N_{\text{H}}/\text{cm}^{-2}) \sim 23$. To consider more heavily obscured cases, we adopt a putative torus model as follows:

```
TBabs*cabs*zpowerlw*zhighect
+zpowerlw*zhighect
*mtable{e - torus_20161121_2500M.fits}
+atable{refl_fe_torus.fits, }
```

represented in XSPEC terminology.¹⁵ This takes account of an absorbed and Compton scattered power-law component, a reflected continuum, and an accompanying fluorescent iron-K α line. The photon index of the power law, inclination, and opening angles of the torus are set to 1.7, 70°, and 60°, respectively. Even under a Compton-thick absorption of $N_{\text{H}} = 1.5 \times 10^{24} \text{ cm}^{-2}$ in the torus equatorial plane, the upper bound of the intrinsic luminosity is still very low with $\log(L_{2-10}/\text{erg s}^{-1}) = 41.75$, or the bolometric luminosity of $\log(L_{\text{bol}}/\text{erg s}^{-1}) = 43.05$. Note that other well-known torus models, such as MYTorus and Borus (Yaqoob 2012; Baloković et al. 2018), also give similar luminosity upper bounds with the difference of a factor of 1.2. Finally, we mention that the X-ray luminosity expected from the star formation in the infrared

(Ueda et al. 2014) is consistent with the 0.5–8 keV upper bound ($\sim 2 \times 10^{41} \text{ erg s}^{-1}$) from the extrapolation based on the 3–8 keV band, where a canonical power-law model seen in star-forming galaxies with $\Gamma = 2.0$ and $3 \times 10^{21} \text{ cm}^{-2}$ (Mineo et al. 2012) is utilized.

3. Discussion

3.1. Very Faint AGN Even if It Is Highly Obscured

Our *NuSTAR* result shows the strongest current luminosity constraints with $\log(L_{\text{bol}}/\text{erg s}^{-1}) < 42.5$ for $\log(N_{\text{H}}/\text{cm}^{-2}) \lesssim 23$, and $\log(L_{\text{bol}}/\text{erg s}^{-1}) < 43.1$ for $\log(N_{\text{H}}/\text{cm}^{-2}) \simeq 24.2$. This indicates that the central engine of Arp 187 is currently very faint even if it is highly obscured by gas. This is consistent with the absence of the AGN torus emission in the *Spitzer*/IRS spectra, which gives us the 3σ upper-bound luminosity of $\log(L_{\text{bol}}/\text{erg s}^{-1}) < 43.8$ (Ichikawa et al. 2016).

One would expect that Arp 187 might be obscured by the thicker absorption of $N_{\text{H}} = 10^{25} \text{ cm}^{-2}$. In this case, the expected upper bound reaches to $\log(L_{2-10}/\text{erg s}^{-1}) = 42.92$, or $\log(L_{\text{bol}}/\text{erg s}^{-1}) = 44.22$, exceeding the upper bound obtained from the *Spitzer*/IRS spectra. However, this situation is unlikely because the reprocessed infrared emission should be observed even in such highly obscured situation, contributing to the *Spitzer*/IRS spectra (e.g., Yan et al. 2019). Thus, we conclude that the central engine of Arp 187 is likely to be dead, even if we consider the Compton-thick level obscuration, and the extreme absorption reaching $N_{\text{H}} = 10^{25} \text{ cm}^{-2}$ is also unlikely.

¹⁵ The FITS files of e-torus models were originally created by Ikeda et al. (2009). The first one is publicly available from <https://heasarc.gsfc.nasa.gov/xanadu/xspec/models/etorus.html>, and the second one was privately obtained from Ikeda et al. (2009).

3.2. The Drastic Luminosity Decline

One important goal of our study is to constrain how rapidly the AGN in Arp 187 has dropped its luminosity. As already described in Section 1, the multiwavelength observations indicate that Arp 187 has experienced a luminosity decline. Figure 2 summarizes the long-term decline together with the X-ray upper bound we have obtained. The luminosity and the lookback time are obtained by combining the observational results of several AGN indicators with different physical scales (Ichikawa et al. 2016, 2019b).

Figure 2 shows that, thanks to its sensitivity in the hard X-ray band, *NuSTAR* (blue point) gives us a nearly two orders of magnitude fainter luminosity constraint than a previous estimate in the *Swift*/BAT 105 month catalog (purple; Oh et al. 2018). In addition, the *NuSTAR* observation gives the constraint on the current luminosity better than the MIR observations. Compared to the luminosity of $\log(L_{\text{bol}}/\text{erg s}^{-1}) = 46.15$ (see the black point) obtained from the NLR tracing the AGN activity 10^{3-4} yr ago, Arp 187 has experienced the luminosity decline at least by a factor of $>10^3$.

Naively, this drastic luminosity experience indicates that the accretion rate in Arp 187 should have drastically dropped over $>10^3$ times within 10^4 yr. This seemingly short timescale itself is consistent with the viscous timescale of the UV emitting region (see the discussion of Ichikawa et al. 2019b). There, however, remains another question of how such a drastic decline of accretion was achieved. A gradual decrease of an external gas supply to the accretion disk cannot produce such a drastic luminosity decline. One suggestion is thus that the accretion disk has a clear outer disk boundary out of which the accretion rate drastically drops over $>10^3$ times. Therefore, one burst-like accretion event is preferable for realizing such a drastic accretion rate change.

3.3. Tidal Disruption Event in Arp 187?

One might argue that a tidal disruption event (TDE) of a star could reproduce such a drastic accretion change. However, there are three difficulties in the case of Arp 187. First, the estimated BH mass of Arp 187 is $6.7 \times 10^8 M_{\odot}$, which thus requires a massive star above the main sequence, such as the red giant, to be tidally disrupted by the tidal field of the SMBH (e.g., Rees 1988). The second is the luminosity problem: even if a red supergiant, whose total mass is typically $\lesssim 50 M_{\odot}$, is tidally disrupted, it would be hard for the large BH ($\sim 7 \times 10^8 M_{\odot}$) to reach the expected Eddington ratio of Arp 187 ($\lambda_{\text{Edd}} \sim 0.1$), or an accretion rate of $\sim 2.5 M_{\odot} \text{ yr}^{-1}$ (e.g., see Figure 5 of MacLeod et al. 2013). Third, the expected timescale: considering the rapid luminosity decline of TDEs that decay roughly as $L \propto t^{-5/3}$, the maximum observable timescale of AGN or quasars would be a maximum of $\lesssim 10$ yr. If a TDE is assumed to have happened at the time of jet launch, or 10^4 – 10^5 yr ago (see Figure 2 or Section 1), the estimated NLR size should be expanded only up to ~ 10 pc scale, and the [O III] would cool on timescales of ~ 100 yr and thus such a feature is no longer observable at the current stage. This is in clear disagreement with the observations, which leads us to exclude a TDE of a star as the origin of the accretion episode currently observed in Arp 187.

The other possibility is the TDE of a giant molecular cloud (GMC). Arp 187 is a good environment to produce such an event because of the star-forming galaxy with plenty gas mass

of $\sim 2 \times 10^9 M_{\odot}$ in the central ~ 900 pc (Ueda et al. 2014). The tidal radius of a GMC cloud is big enough as $R_{\text{TDE}} = 200 \times (R_{\text{GMC}}/20 \text{ pc}) \times (M_{\text{BH}}/10^8 M_{\odot})^{1/3} \times (M_{\text{GMC}}/10^5 M_{\odot})^{-1/3} \text{ pc}$, where a canonical range of GMC radii is $R_{\text{GMC}} = 10$ – 50 pc and that of GMC masses is $M_{\text{GMC}} = 10^4$ – $10^6 M_{\text{Sun}}$ in local galaxies (e.g., Bolatto et al. 2008). Although this idea is exclusively applied to Sgr A* (e.g., Bonnell & Rice 2008) and further theoretical studies are required to examine the case of much bigger SMBHs with $M_{\text{BH}} > 10^8 M_{\odot}$, a GMC with mass of $\sim 10^6 M_{\odot}$ can feed the SMBH of Arp 187 with the sub-Eddington level for $M_{\text{GMC}}/(2.5 M_{\odot} \text{ yr}^{-1}) \sim 4 \times 10^5 \text{ yr}$. This would be long enough to produce the expected-size NLR by keeping the estimated past luminosity of $\log(L_{\text{bol}}/\text{erg s}^{-1}) \simeq 46.15$.

3.4. Accretion Disk Outer Boundary after Nuclear Starburst

Our observation indicates the rapid luminosity decline in the final phase of quasar activity in Arp 187. One question raised from this result is whether this drastic luminosity decline is a unique event only for Arp 187 or a rather common behavior in the final phase of quasars.



Once the accretion rate somehow exceeds a certain value, it may naturally produce the drastic accretion rate gap, resulting in the drastic luminosity decline in the final phase of a quasar. By utilizing the nuclear starburst disk model by Thompson et al. (2005), Ballantyne (2008) and Inayoshi & Haiman (2016) discussed such a possibility that once the rapid accretion rate of $>10 M_{\odot} \text{ yr}^{-1}$ is achieved, at around ~ 1 – 10 pc, vigorous star formation starts to deplete most of the gas and the accretion rate rapidly decreases by a factor of $\sim 10^{2-3}$ times at some point, making a strong accretion rate gap. This is in good agreement with our expectation of the clear outer accretion disk boundary.

Considering that Arp 187 is a merger remnant, such a rapid accretion flow with $>10 M_{\odot} \text{ yr}^{-1}$ could be achieved by a previous major merger (e.g., Hopkins & Quataert 2010). The expected lifetime of such an accretion disk is $t_{\text{life}} \sim t_{\text{vis}}(r = 1 \text{ pc}) \sim 5 \times 10^7 \text{ yr}$, which is long enough to produce the NLR and is actually consistent with the typical quasar lifetime (e.g., Martini 2004). Based on those indirect observational signatures, quasars that experienced a drastic accretion inflow might follow the same luminosity decline in their future after consuming most of the gas in the accretion disk. On the other hand, a smooth accretion that has never exceeded the critical accretion rate of $\sim 10 M_{\odot} \text{ yr}^{-1}$ will show more slower luminosity decline longer than $\sim 10^4 \text{ yr}$.

We acknowledge the anonymous referee for helpful suggestions that strengthened the Letter. We thank Mitsuru Kokubo, Ryo Tazaki, and Takuma Izumi for fruitful discussion. This work is supported by Program for Establishing a Consortium for the Development of Human Resources in Science and Technology, Japan Science and Technology Agency (JST) and is partially supported by Japan Society for the Promotion of Science (JSPS) KAKENHI (18K13584, K.I.; 18J01050 and 19K14759, Y.T.; 17K05384, Y.U.). T.K. was financially supported by the Grant-in-Aid for JSPS Fellows for young researchers (PD). C.R. acknowledges support from the CONICYT+PAI Convocatoria Nacional subvencion a instalacion en la academia convocatoria año 2017 PAI77170080.

Facility: *NuSTAR*.

ORCID iDs

Kohei Ichikawa  <https://orcid.org/0000-0002-4377-903X>
 Taiki Kawamuro  <https://orcid.org/0000-0002-6808-2052>
 Claudio Ricci  <https://orcid.org/0000-0001-5231-2645>
 Hyun-Jin Bae  <https://orcid.org/0000-0001-5134-5517>
 Kenta Matsuoka  <https://orcid.org/0000-0002-2689-4634>
 Yoshiki Toba  <https://orcid.org/0000-0002-3531-7863>
 Yoshihiro Ueda  <https://orcid.org/0000-0001-7821-6715>

References

- Asmus, D., Gandhi, P., Hönig, S. F., Smette, A., & Duschl, W. J. 2015, *MNRAS*, **454**, 766
- Ballantyne, D. R. 2008, *ApJ*, **685**, 787
- Baloković, M., Brightman, M., Harrison, F. A., et al. 2018, *ApJ*, **854**, 42
- Bennert, N., Falcke, H., Schulz, H., Wilson, A. S., & Wills, B. J. 2002, *ApJL*, **574**, L105
- Bolatto, A. D., Leroy, A. K., Rosolowsky, E., Walter, F., & Blitz, L. 2008, *ApJ*, **686**, 948
- Bonnell, I. A., & Rice, W. K. M. 2008, *Sci*, **321**, 1060
- Burtscher, L., Meisenheimer, K., Tristram, K. R. W., et al. 2013, *A&A*, **558**, A149
- Dai, X., Kochanek, C. S., Chartas, G., et al. 2010, *ApJ*, **709**, 278
- Forster, K., Harrison, F. A., Dodd, S. R., et al. 2014, *Proc. SPIE*, **9149**, 91490R
- Hopkins, P. F., Hernquist, L., Cox, T. J., et al. 2006, *ApJS*, **163**, 1
- Hopkins, P. F., & Quataert, E. 2010, *MNRAS*, **407**, 1529
- Ichikawa, K., Packham, C., Ramos Almeida, C., et al. 2015, *ApJ*, **803**, 57
- Ichikawa, K., Ricci, C., Ueda, Y., et al. 2017, *ApJ*, **835**, 74
- Ichikawa, K., Ricci, C., Ueda, Y., et al. 2019a, *ApJ*, **870**, 31
- Ichikawa, K., Ueda, J., Bae, H.-J., et al. 2019b, *ApJ*, **870**, 65
- Ichikawa, K., Ueda, J., Shidatsu, M., Kawamuro, T., & Matsuoka, K. 2016, *PASJ*, **68**, 9
- Ichikawa, K., Ueda, Y., Terashima, Y., et al. 2012, *ApJ*, **754**, 45
- Ikeda, S., Awaki, H., & Terashima, Y. 2009, *ApJ*, **692**, 608
- Inayoshi, K., & Haiman, Z. 2016, *ApJ*, **828**, 110
- Kawamuro, T., Schirmer, M., Turner, J. E. H., Davies, R. L., & Ichikawa, K. 2017, *ApJ*, **848**, 42
- Kawamuro, T., Ueda, Y., Tazaki, F., Ricci, C., & Terashima, Y. 2016, *ApJS*, **225**, 14
- Keel, W. C., Lintott, C. J., Maksym, W. P., et al. 2017, *ApJ*, **835**, 256
- King, A. 2016, *MNRAS*, **456**, L109
- Kormendy, J., & Ho, L. C. 2013, *ARA&A*, **51**, 511
- Lansbury, G. B., Stern, D., Aird, J., et al. 2017, *ApJ*, **836**, 99
- MacLeod, M., Ramirez-Ruiz, E., Grady, S., & Guillochon, J. 2013, *ApJ*, **777**, 133
- Marconi, A., Risaliti, G., Gilli, R., et al. 2004, *MNRAS*, **351**, 169
- Martini, P. 2004, in *Coevolution of Black Holes and Galaxies*, ed. L. C. Ho (Cambridge: Cambridge Univ. Press), 169
- Mineo, S., Gilfanov, M., & Sunyaev, R. 2012, *MNRAS*, **419**, 2095
- Morgan, C. W., Kochanek, C. S., Morgan, N. D., & Falco, E. E. 2010, *ApJ*, **712**, 1129
- Mortlock, D. J., Warren, S. J., Venemans, B. P., et al. 2011, *Natur*, **474**, 616
- Natarajan, P., & Treister, E. 2009, *MNRAS*, **393**, 838
- Netzer, H. 2003, *ApJL*, **583**, L5
- O'Dea, C. P. 1998, *PASP*, **110**, 493
- Oh, K., Koss, M., Markwardt, C. B., et al. 2018, *ApJS*, **235**, 4
- Rees, M. J. 1988, *Natur*, **333**, 523
- Ricci, C., Trakhtenbrot, B., Koss, M. J., et al. 2017, *ApJS*, **233**, 17
- Sartori, L. F., Schawinski, K., Trakhtenbrot, B., et al. 2018, *MNRAS*, **476**, L34
- Schawinski, K., Koss, M., Berney, S., & Sartori, L. F. 2015, *MNRAS*, **451**, 2517
- Schirmer, M., Diaz, R., Holhjem, K., Levenson, N. A., & Winge, C. 2013, *ApJ*, **763**, 60
- Soltan, A. 1982, *MNRAS*, **200**, 115
- Thompson, T. A., Quataert, E., & Murray, N. 2005, *ApJ*, **630**, 167
- Toba, Y., Oyabu, S., Matsuhara, H., et al. 2014, *ApJ*, **788**, 45
- Ueda, J., Iono, D., Yun, M. S., et al. 2014, *ApJS*, **214**, 1
- Ueda, Y., Hashimoto, Y., Ichikawa, K., et al. 2015, *ApJ*, **815**, 1
- Vasudevan, R. V., Mushotzky, R. F., Winter, L. M., & Fabian, A. C. 2009, *MNRAS*, **399**, 1553
- Villar-Martín, M., Cabrera-Lavers, A., Humphrey, A., et al. 2018, *MNRAS*, **474**, 2302
- Wylezalek, D., Zakamska, N. L., Greene, J. E., et al. 2018, *MNRAS*, **474**, 1499
- Yan, W., Hickox, R. C., Hainline, K. N., et al. 2019, *ApJ*, **870**, 33
- Yaqoob, T. 2012, *MNRAS*, **423**, 3360